Estimation of Source Parameter of Microseismic Events with Large Magnitude Collected at Basel, Switzerland in 2006

Yusuke Mukuhira[1], Hiroshi Asanuma[1], Hiroaki Niitsuma[1], Markus Häring[2], and Nicholas Deichmann[3]

[1]Graduate School of Environmental Studies, Tohoku University (Japan)
[2]Geothermal Explorer Ltd. (Switzerland)
[3]Swiss Seismological Service (SED) (Switzerland)

Keywords

Microseismicity, magnitude, HDR, HWR, HFR, stimulation, Basel

ABSTRACT

Occurrence of microseismic events with large magnitude, which are felt on the surface, has been recently receiving much attention as one of the practical problems in stimulation/production of HDR/HFR/EGS geothermal reservoirs. The microseismic activities with large magnitude have been also reported from some of the hydrothermal geothermal fields.

Microseismic events with moment magnitude Mw exceeded 2.0 occurred in deeper and middle part of the microseismic cloud during and just after a hydraulic stimulation at Basel, Switzerland, in 2006. Three more large events (Mw>2.0) occurred in shallower part of the seismic cloud by within two months from the bleeding-off. Because of the occurrence of the large events, the project at Basel has been terminated.

The authors estimated some of the seismic source parameters (fault plane solution, seismic moment, size of ruptured area, average slip along fault, and stress drop) of the large events to understand the nature of the shear slip on fractures. Spatial distribution of the hypocenter and the fault plane solution (FPS) showed that most of the FPS of the large events had nearly N-S azimuth and those for small events had NW-SE azimuth. Most of the estimated stress drops were less than 1.0MPa, while some of the large events had larger stress drop. Events with higher stress drop (>1.0MPa) showed a linear relationship between the seismic moment and the ruptured area, suggesting that "scaling law" in natural seismology stands for this data set. Observational facts indicated that control factor of the magnitude is not simply either the size of the fault area or the stress drop.

Introduction

Recently recognized practical problem in subsurface development which includes HDR/HFR/EGS development, geothermal production from hydrothermal reservoir, CCS, and EOR is the occurrence of microseismic events with large magnitude (Majer et al., 2007, Roger and Charles, 1982, Suckale, 2010). Large events during and after the stimulation of HDR/HFR/EGS reservoirs has been observed at Soultz (France), Cooper Basin (Australia), and Basel (Switzerland) (Asanuma et al., 2005, Baria et al., 2005), and some degree of damages to buildings and infrastructure in urbanized area has been reported (Deichmann et al., 2009).

Microseismic activity has been considered as one of the evidences of human-induced shear slip to improve permeability in the reservoirs. It has been interpreted in seismology that there is a strong correlation between the magnitude of the natural earthquakes and the size of the rupture zone. However, relationship between the magnitude of the microseismic events and improvement of the permeability/productivity of the geothermal reservoirs has not been well understood. Moreover, there is some possibility that people consider large event as an earthquake and may have misunderstanding that geothermal development increases the risk of natural earthquake. Hence, a clear understanding of the physics behind the large microseismic events is needed, and technologies for "soft stimulation" must be developed. Research to investigate the characteristics of the events has been undertaken by researchers worldwide (e.g., Bromley, 2005; Majer et al., 2007).

Geothermal Explorers Ltd. (GEL), operating for Geopower Basel AG, started development of a co-generation system of electrical power and heating energy (3MWe and 20MWt) at Basel, Switzerland, in 1996. GEL drilled a deep borehole (Basel-1) into granitic basement, and carried out the first hydraulic stimulation in December 2006. A total amount of 11,500m^3 of fresh water was injected into the openhole section of the borehole over a stimulation period of six days (Häring et al., 2008). Seismic events with moment magnitude (Mw) greater than 2.0 occurred in the deep and mid-depth parts of the seismic cloud during and just after the hydraulic stimulation. Three more large events (Mw>2.0) occurred in the shallow part of the seismic cloud by two months after the bleeding-off. Because of these large events, the Basel project was suspended for risk analysis and finally terminated.

The authors have previously concluded that most of the large events from the mid-depth and deep parts of the seismic cloud originated in ruptures involving single/multiple asperities (Mukuhira et al., 2008). It has been also concluded that the large events in the shallow part of the seismic cloud occurred in fractures which were sub-parallel to the stimulated zone, because their hypocenters were spatially independent to the main seismic cloud and trace had lower similarity to those inside the main seismic cloud. We have also found that the critical pore pressure for shear slip of the large events is relatively low and the most of large events occurred in the area where the increase of pore pressure from hydrostatic condition was also relatively low. These observational facts suggest that local concentration of critical pore pressure is not the trigger of the large events at Basel, and the re-distribution of stress or decrease in the coefficient of friction can be the trigger of the large events (Mukuhira et al, 2009).

In this paper, we describe results of estimation of some of the source parameters (fault plane solution, seismic moment, size of rupture area, average slip along fault, and stress drop), and discuss characteristics of the shear slip on a fracture which induced the large events.

Outline of the Stimulation and Microseismic Monitoring

The hydraulic stimulation at Basel was achieved by pumping a total of 11,500m^3 of water into a 4750m true vertical distance (TVD) borehole (Basel-1) over six days. The entire open-hole section (from 4379 to 4750m TVD), which includes some pre-existing natural permeable zones, was pressurized. The maximum wellhead pressure was around 30MPa at a flow rate of 50L/s (Ulrich et al., 2007).

The microseismic monitoring network, which consisted of six permanent seismometers and one temporary seismometer placed in boreholes, detected more than 13,000 possible microseismic events during and after the stimulation period (up to February, 2008). The number of events located by conventional absolute mapping technique was around 2,900 (Asanuma et al., 2007). Distribution of the hypocenters showed a sub-vertical planar structure with an approximately NNW–SSE azimuth, which is consistent with the horizontal maximum stress around Basel region. Dominant source mechanisms, which were estimated by Swiss Seismological Service (SED) for 28 of the larger events, were strike-slip movement on sub-vertical fractures with N–S azimuth (Deichmann et al., 2007). Asanuma et al. (2008) showed that the hydraulic injection stimulated several sub-vertical fractures (or thin fracture networks) with NNW–SSE azimuth and a horizontal extent of 200–400m. Because there is no common definition of the large event, we defined large event as a microseismice event whose moment magnitude Mw exceed 2.0 in this study.

Estimation of Source Parameter

a) Methodology

Fault Plane Solution

Fault plane solutions (FPS) for 28 larger events which were detected by a surface earthquake monitoring network were estimated by SED (Deichmann et al., 2007) on the basis of P-wave polarity. SED also determined the local magnitude M_L of these 28 events to be within a range from M_L=1.7 to 3.4. We calculated critical pore pressure for shear slip for a pair of conjugate fault planes which were determined by FPS using tectonic stress state. One of the pair of fractures which had smaller pore pressures was identified as an actually slipped fracture. We selected one of the fractures whose critical pore pressure for shear slip is smaller (Mukuhira et al., 2009). We also estimated fault planes for the smaller events, of which FPSs were not estimated by SED, from the orientation of seismic structure of the microseismic multiplets. This is because Asanuma et al., (2008) reported that the multiplet clusters identified in high-frequency at Basel are strongly correlated to the existing microscopic fracture system.

Seismic Moment, Size of Rupture Area, Average Slip Along Fault, and Stress Drop

The seismic moment, size of ruptured area, average slip along fault, and stress drop can be estimated from spectra of the microseismic events following a model proposed by Brune (1970). The researchers in Tohoku University have previously decided to use the traces detected at Riehen-2 station, one of the deep monitoring stations, to estimate the spectrum, because signal to noise ratio, bandwidth, and radiation angle from the possible fractures are most suitable (Asanuma et al., 2008). Velocity spectra were estimated from signals just after arrival of S wave, and they were converted to displacement spectra. The observational source spectrum was obtained after compensating attenuation using equation (1).

$$S_{obs}(f) = \Omega(f) \cdot e^{\pi f t/Q} \tag{1}$$

$S_{obs}(f)$: Observational source spectrum, $\Omega(f)$: Observational spectrum of displacement, t: Travel time from the source to the sensor, Q: Quality factor

Equation (2) shows the theoretical source spectrum from Brune's model. Theoretical source spectrum is determined by two parameters, corner frequency and long period amplitude.

$$S_{theo}(f) = \frac{\Omega_0}{\left[1+(f/f_c)^{\gamma n}\right]^{1/\gamma}} \tag{2}$$

$S_{theo}(f)$: Theoretical source spectrum, Ω_0: Long period amplitude, f_c: Corner frequency, $n = 2$, $\gamma = 2$

The estimates of the corner frequency f_c, the long period amplitude Ω_0, and the quality factor Q can obtained by fitting $S_{obs}(f)$ to $S_{theo}(f)$ using a least mean square algorism in equation (3) (Fehler and Phillips, 1991).

$$m = \sum_{i=1}^{N}\sum_{j=1}^{M}[\log(S_{theo,i}(f_j)) - \log(S_{obs,i}(f_j))]^2 \tag{3}$$

m: Misfit, N: Number of the events, M: Maximum frequency (100Hz, in this study),

The relationship among seismic moment, source radii, and stress drop is represented by corner frequency and long time amplitude as shown in equation (4).

$$M_O = 4\pi\rho\beta^3 \cdot \frac{r}{R^S}\Omega_0 \tag{4}$$

M_O: Seismic moment, ρ: density (2.75g/cm^3, in this study), β: S wave velocity (3450m/s, in this study), r: Source-sensor distance, R^S: Radiation pattern for S wave

The seismic moment can be converted into moment magnitude M_W by equation (5).

$$M_W = \left(\frac{\log M_O}{1.5}\right) - 10.73 \tag{5}$$

Source radius R is obtained using Madoriaga's model (Madoriaga, 1976).

$$R = \frac{k\beta}{f_c} \tag{6}$$

k : Constant (0.32 for P wave, 0.21 for S wave)

The stress drop $\Delta\sigma$ is calculated from the seismic moment and the source radius using equation (7).

$$\Delta\sigma = \frac{7}{16R^3} M_O \tag{7}$$

b) Results of the Estimation of Source Parameters

Spatial distribution of fault planes for large events and some of the microseismic events with high stress drop (>1MPa) is shown in Figure 1. We found that most of the fault planes of the large events have N-S azimuth, and the source radii of the large events and the smaller events crossed each other. Figure 2 shows lower hemisphere projection of the pole of the identified fracture planes of deep large events and multiplet planes nearby. The pole of conjugate pairs of the "most slip-able fractures" at stress state at Basel is also plotted. It can be observed that there is different distribution of the pole of the fault planes for the deep large events and surrounding smaller events.

Figure 3 shows some examples of the fitting of spectra for Q=500. The theoretical and observational source spectra showed reasonable consistency. A histogram of estimated moment magnitude is shown in Figure 4. Some of the microseismic events whose moment magnitude is larger than 2.0, showed some misfit to the Gutenberg-Richter law.

A relationship between the corner frequency and the seismic moment is shown in Figure 5, where clear correlation between the corner frequency and the -3rd power of the seismic moment is observed.

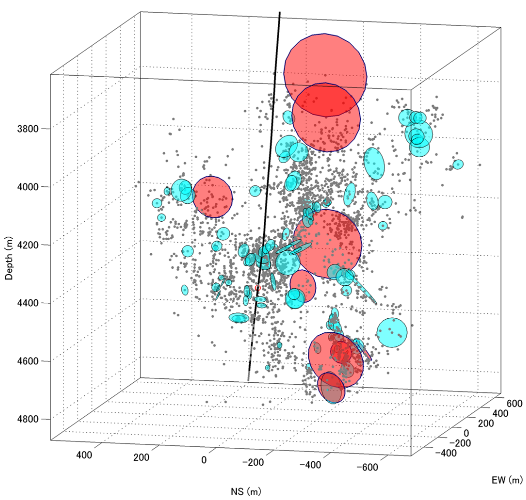

Figure 1. Spatial distribution of the FPS with source radii for large event (Mw>2.0) and events with high stress drop (> 1MPa). Black line indicates the trace of the injection well. Red circles indicate large event and blue circles indicate events with high stress drop.

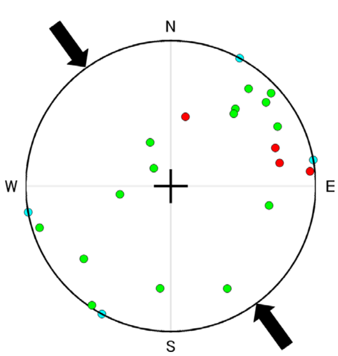

Figure 2. Lower hemisphere projection of poles of identified fracture planes for deep large events and microseismic multiplet structures. Red circles show the poles of fracture planes for large events whose hypocentral depth is deeper than 4500m. Green circles indicate the poles of the multiplet structure deeper than 4500m. Arrows show the azimuth of the maximum horizontal stress (N 144° E). Blue circles show the pole of conjugate pair of the "most slip-able fractures" to the stress state at Basel.

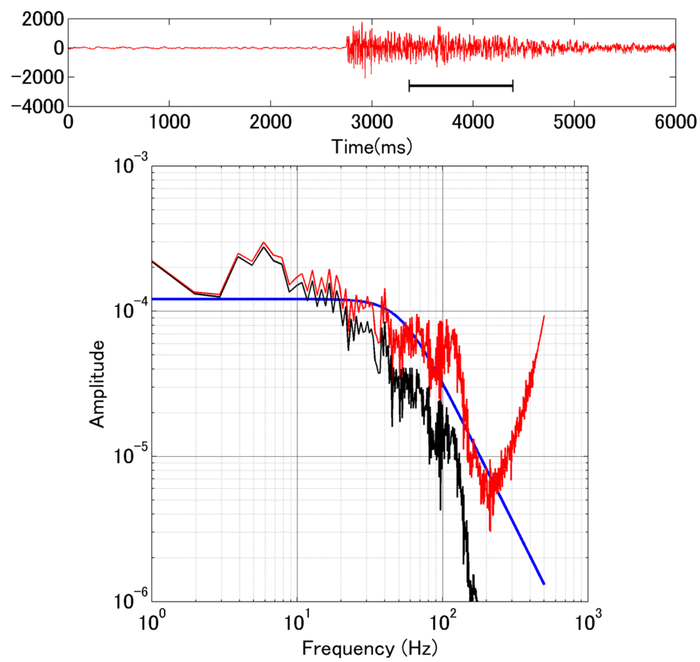

Figure 3. An example of waveform of microseismic event with Mw of 0.75 and observational/theoretical source spectra. Black line: the original displacement spectrum, red line: observational source spectrum, and blue line: theoretical source spectrum.

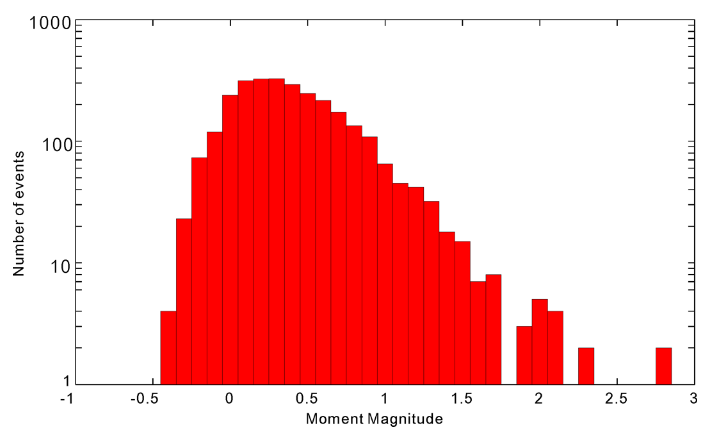

Figure 4. Histogram of the moment magnitude estimated in this study.

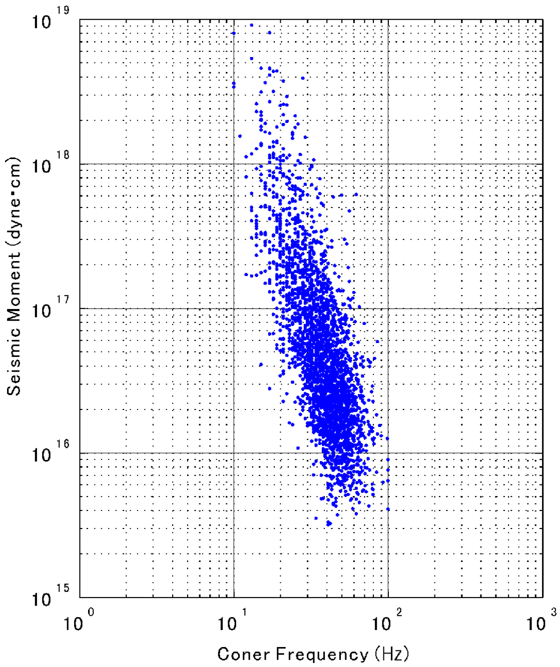

Figure 5. Relationship between the corner frequency and the seismic moment.

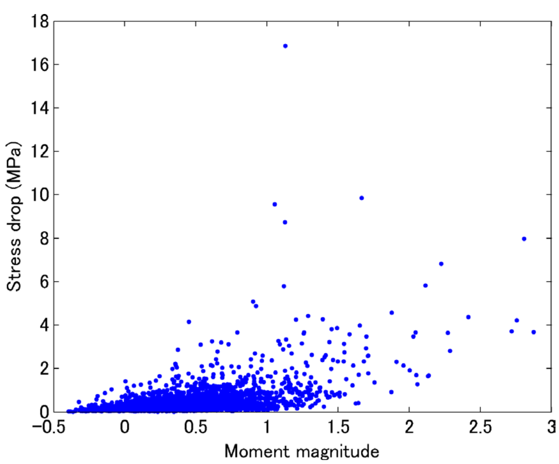

Figure 6. Relationship between the moment magnitude and the stress drop.

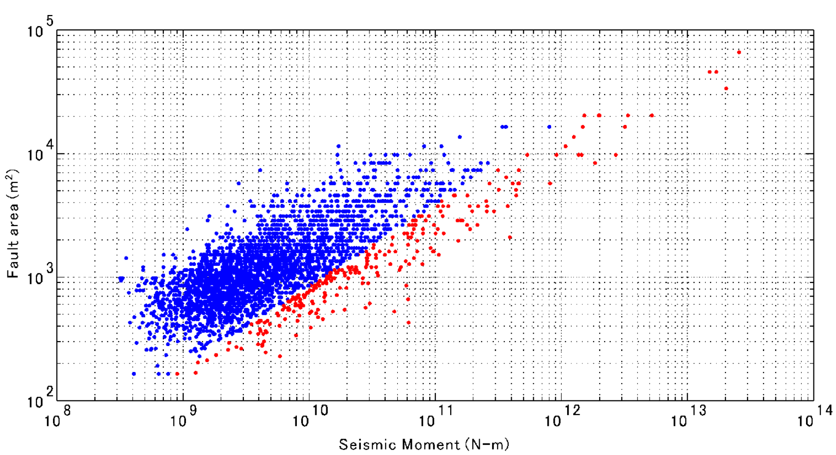

Figure 7. Correlation between the seismic moment and the fault area in log scale. Red dots indicate events with high stress drop (> 1.0MPa).

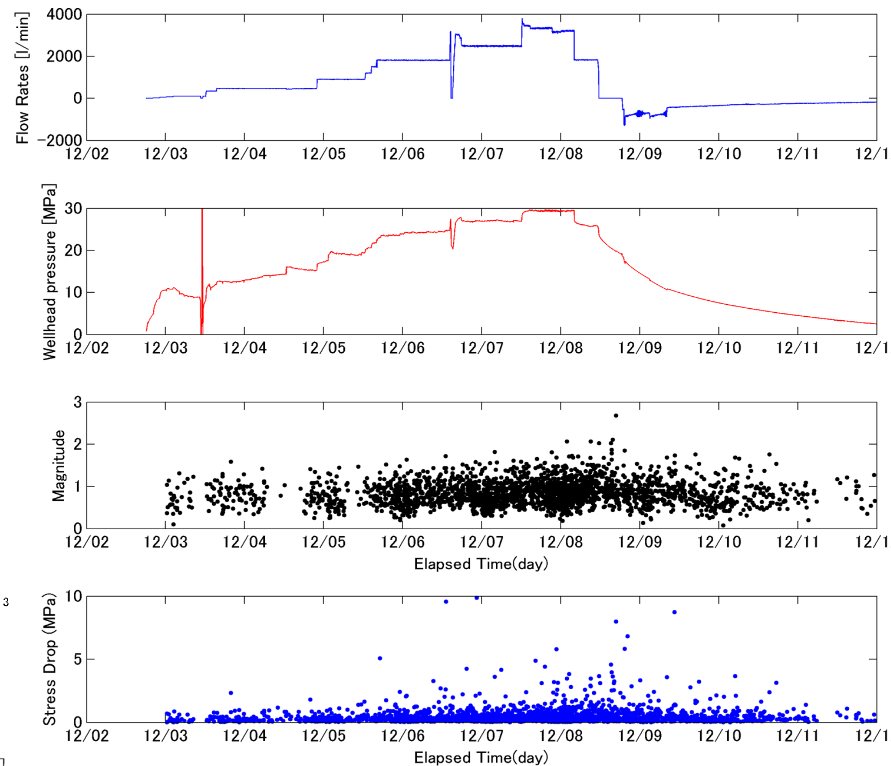

Figure 8. Time series of the stress drop and the moment magnitude.

Relationship between the moment magnitude and the stress drop is shown in Figure 6. Stress drop for most of the microseismic events is less than 1.0MPa and stress drop has a trend that it increases with the moment magnitude. Figure 7 shows correlation between the seismic moment and the fault area, where the red dots represent the microseismic events whose stress drop is larger than 1.0MPa.

Time series and spatial distribution of the stress drop are plotted in Figures 8 and 9. Spatial distribution of events with high stress drop (>1.0MPa) is shown with colored marks in Figure 9. Microseismic events with high stress drop show weak correlation to the stimulation. Events with high stress drop widely distributed within the seismic cloud, especially in the area where 4 deep large events occurred (-400<NS<-200, 4600<depth<4800). We also identified one area where events with high stress drop occurred around the one of the main feed points (-200<NS<0, 4200<depth<4300), even no large event occurred.

Discussion

Asanuma et al., (2008) have reported that the fracture system around the stimulated zone in Basel can be modeled by a mesh-like fracture network (Hill, 1977), where the reservoir consists of conjugate pairs of the "most slip-able fractures" to a given stress state. This is because the azimuth of the multiplet seismic structures distributed within ±30 degrees to the maximum horizontal stress. The conjugate pair of the "most slip-able fractures" at Basel has azimuth of N-S (N 170° E) and NW-SE (N 118° E) considering the stress state. As seen in Figure 2, most of the large events in the deep part of the stimulated zone occurred from one of the conjugate

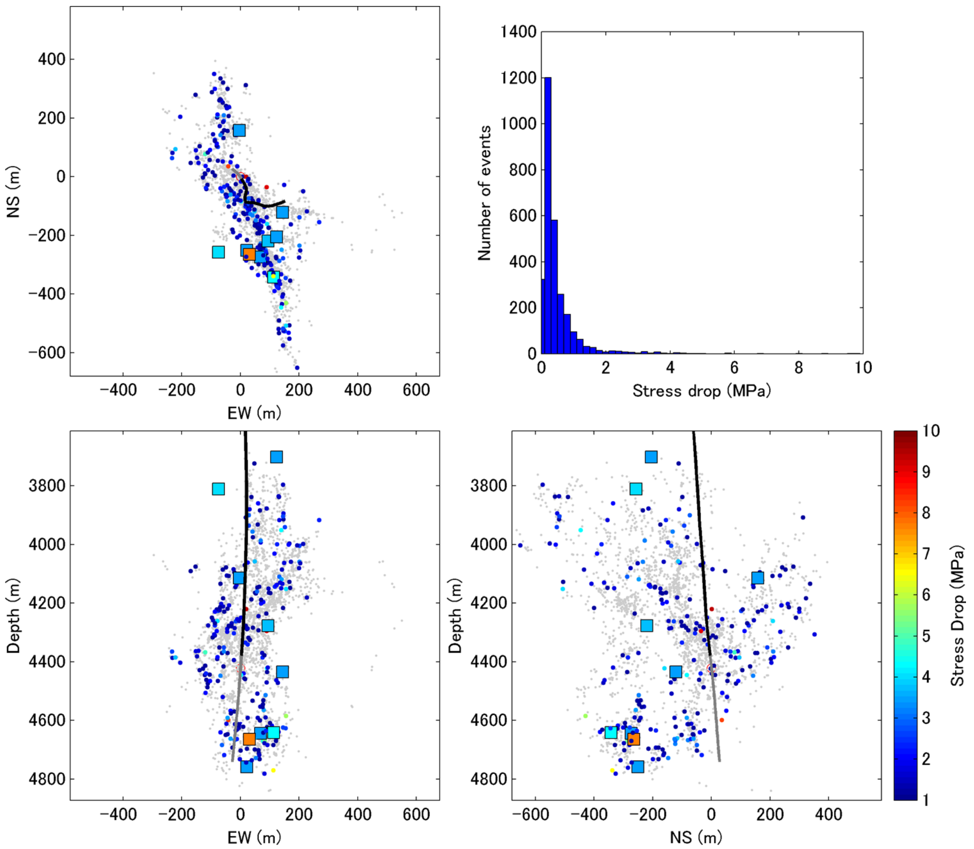

Figure 9. Spatial distribution of the events with high stress drop (>1.0MPa). Color contour indicates the stress drop. Squares show the hypocenter of the large event (Mw>2.0).

fracture planes which has nearly N-S azimuth. The azimuth of the fracture planes for smaller events more widely distributed to the conjugate fractures. These results are consistent with our previous results that critical pore pressure for the large events is lower than the surrounding events with smaller magnitude. The reason why the large events mainly occurred on only one of the conjugate pair of the fractures is currently unknown.

Linearity between the corner frequency and the -3rd power of the seismic moment was observed in the data set collected at HDR site in Fenton Hill (Fehler and Phillips, 1991) and Ogachi, and some mine fields (Gibowicz, 1995) as well as natural earthquakes. Therefore, we understand the estimated corner frequency and seismic moment are reasonable and peculiar phenomena related to source parameter have not occurred at Basel.

Large events and other smaller events showed liner relationship between their seismic moment and fault area. A hypothesis that unusual stress concentration on small fractures brought the large event can be eliminated. However, spatial distribution of the stress drop showed that the deep large events occurred in an area (-400<NS<-200, 4600<depth<4800) where considerable number of events with high stress drop occurred. Such trend has been also observed in the data collected at Soutlz (Michelet et al., 2004). This result shows a possibility of re-distribution of the stress associated with stimulation. In Soultz, events with high stress drop were mainly observed after shut in (Michelet et al., 2004). However, such trend was not observed in the data from Basel.

Conclusions

We estimated some of the source parameters of microseismic events collected during and after the hydraulic stimulation at Basel in 2006. The fault plane solution of the large events showed N-S azimuth, suggesting that they occurred on one of the conjugate pair of fractures which have the smallest critical pore pressure for shear slip. We estimated corner frequency and long period amplitude using Brune's model, and calculated seismic moment, source radii, and stress drop. Evaluation of source parameter revealed that the large events follow the "scaling law" and it is unlikely that they occurred on fractures with peculiar stress drop or rupture velocity. Spatial distribution of the stress drop revealed that most of the large events which were observed just after the stimulation occurred in a region where the events with small magnitude had relatively higher stress drop.

The characteristics of the large events observed at Basel have been more clearly understood and some unknown points, especially on triggering mechanism and control factor of the magnitude, were found out throughout this study. Further investigation on stress re-distribution, change in the friction coefficient associated with stimulation will be carried out by the authors.

Acknowledgements

We thank Geopower Basel AG for the provision of the microseismic data set and the approval to publish these post processing results. This study was supported in part by Ministry of Education, Culture, Sports, Science and Technology and Japan Society for the Promotion of Science.

References

Asanuma H., H. Nozaki, H. Niitsuma, and D. Wyborn, 2005. "Interpretation of microseismic events with larger magnitude collected at Cooper Basin, Australia" *Geothermal Resources Council Transactions*, v. 29, p. 87-91.

Asanuma H., Y. Kumano, A. Hotta, H. Niitsuma, U. Schanz, and M. Haring, 2007. "Analysis of microseismic events from stimulation at Basel, Switzerland" *Geothermal Resources Council Transactions*, v. 31, p. 265-270.

Asanuma H., Y. Kumano, H. Niitsuma, U. Schanz, and M. Haring, 2008. "Interpretation of reservoir structure from super-resolution mapping of microseismic multiplets from stimulation at Basel, Switzerland in 2006" *Geothermal Resources Council Transactions*, v. 32, p. 65-70.

Baria R., S. Michelet, J. Baumgaertner, B. Dyer, A. Gerard, T. Hettkamp, D. Teza, N. Soma, H. Asanuma, and J. Garnish, 2005. "Creation and Mapping of 5000 m deep HDR/HFR Reservoir to Produce Electricity" *Proceedings of the World Geothermal Congress 2005*, CD-ROM.

Bromley C., 2005. “Advances in environmental management of geothermal developments”, *Proceedings of the World Geothermal Congress 2005*, CD-ROM.

Deichmann N., J. Ernst, and S. Wöhlbier, 2007. “Data analysis. In: Evaluation of the induced seismicity in Basel 2006/2007: locations, magnitudes, focal mechanisms, statistical forecasts and earthquake scenarios” *Report of the Swiss Seismological Service to Geopower Basel AG*.

Deichmann N., and J. Ernst, 2009. “Earthquake focal mechanisms of the induced seismicity in 2006 and 2007 below Basel (Switzerland)” *Swiss Journal of Geosciences* 102 (3).

Fehler M and S. Phillips, 1991. “Simultaneous inversion for Q and source parameters of microearthquakes accompanying hydraulic fracturing in granitic rock”, *Bull. Seism. Am*, v. 81, p. 553-575.

Gibowicz S. J., 1995. “Scaling relations for seismic events induced events induced by mining”, *PEGEOPH*, v. 144, p. 191-209.

Häring M. O., U. Schanz, F. Ladner, and B. Dyer, 2008. “Characterization of the Basel-1 enhanced geothermal system” *Geothermics*, v. 37, p. 469-495.

Hill D. P., 1977. “A model for earthquake swarms” *J.Geophys. Res.*, v. 82, p. 1347-1352.

Madoriaga R., 1976. “The dynamics of an expanding circularfault”, *Bull. Seism. Soc. Am.* v. 66, p. 639-666.

Majer E., R. Baria, M. Stark, S. Oates, J. Bommer, B. Smith, and H. Asanuma, 2007. “Induced seismicity associated with enhanced geothermal systems” *Geothermics*, v. 36, p. 185-222.

Moriya H., H. Niitsuma, and R. Baria, 2005. “Multiplet analysis for estimation of critical pore-pressure of fractures inside geothermal reservoir” *Proceedings of the World Geothermal Congress 2005*, (CD-ROM).

Michelet S., R. Baria, J. Baumgaertner, A. Gérad, S. Oates, T. Hettkamp, and D. Teza, 2004. ”Seismic source parameter evaluation and its importance in the development of an HDR/EGS system”, In: Twenty-ninth workshop on geothermal reservoir engineering. Stanford University; 2004.

Mukuhira Y., H. Asanuma, H. Niitsuma, U. Schanz, and M. Häring. 2008. “Characterization of microseismic events with larger magnitude collected at Basel, Switzerland in 2006” *Geothermal Resources Council Transactions*, v. 32, p. 87-94.

Mukuhira Y., H. Asanuma, H. Niitsuma, U. Schanz, and M. Häring. 2009. “Investigation of relationship of pore pressure to large microseismic events with large collected at Basel, Switzerland in 2006”, *Geothermal Resources Council Transactions*, v. 33, p. 331-335.

Roger P. D., and G. B. Charles, 1982. “Reservoir conditions related to induced seismicity at the Geysers steam reservoir, northern California”, *Bull. Seism. Soc. Am.* v. 72, p. 1317-1327.

Suckale J., 2009. “Induced seismicity in hydrocarbon fields” *Advances in Geophysics*, v. 51, p. 55-106.

Ulrich S., B. Dyer, F. Ladner, and M. O. Häring, 2007. “Part 2: Microseismic aspects of the Basel 1 geothermal reservoir” 5th Swiss Geoscience Meeting, Genova 2007 (Website: http://www.geothermal.ch/english/downloads.html)

Valley B., and K.F. Evans, 2006. “Stress orientation at the Basel geothermal site from wellbore failure analysis in BS1” Report to Geopower Basel AG for Swiss Deep Heat Mining Project Basel. *ETH Report Nr. ETH 3465/56*. Ingenieurgeologie ETH Zürich, Switzerland, p. 29.

Yeo I. W., M. H. De Freitas, and R. W. Zimmerman, 1998. “Effect of shear displacement on the aperture and permeability of a rock fracture” *International Journal of Rock Mechanics and Mining Sciences*, v. 35, p. 1051–1070.